RSC Advances

PAPER

View Article Online
View Journal | View Issue

Cite this: *RSC Adv.*, 2022, **12**, 34724

Preparation and properties of CS/P(AM-*co*-AA) composite hydrogels by frontal polymerization of ternary DES

Bin Li,[a] Wenrui Hao,[a] Peng Wang,*[b] Mengjing Zhou,[a] Jizhen Liu,[c] Zhigang Hu[a] and Ming Ma[a]

A deep eutectic solvent (DES) was prepared from choline chloride (ChCl), acrylamide (AM) and acrylic acid (AA); chitosan (CS) was used as a filler, and CS/P(AM-*co*-AA) composite hydrogels were prepared by frontal polymerization (FP). The hydrogels were characterized by Fourier transform infrared spectroscopy (FTIR) and scanning electron microscopy (SEM). The mechanical properties, pH responsiveness and conductivity of the hydrogel were studied. The results showed that the mechanical properties of the hydrogel were significantly improved by adding CS, and the tensile strength and compressive strength were increased by 11.61 and 1.65 times respectively due to the increase in number of hydrogen bonds. At the same time, due to the presence of AA, the composite hydrogel has excellent pH response and super high swelling performance under alkaline conditions. The introduction of CS enhanced the conductivity of the hydrogel and gradually increased with the increase of CS content. The conductivity of the hydrogel with CS content of 10 wt% was nearly 160 times that of the hydrogel without CS. In this study, a more convenient and rapid method was proposed to prepare conductive composite hydrogels with excellent mechanical properties and pH responsiveness.

Received 4th October 2022
Accepted 23rd November 2022

DOI: 10.1039/d2ra06232a

rsc.li/rsc-advances

1. Introduction

A hydrogel is a three-dimensional network polymer formed by chemical bond crosslinking,[1] which has good hydrophilicity. When placed in water, it will absorb a large number of water molecules and expand. It has a wide application potential in the biomedical field.[2] Because hydrogels are soft and can keep a certain shape, they can be widely used in drought resistance,[3] food detection,[4] biomedicine,[5] biosensors[6] and other fields. According to the different bonding methods of functional groups in the gel network, hydrogels can be divided into physical hydrogels (hydrogen bonds and electrostatic interactions)[7–9] and chemical hydrogels (covalent bonds).[10]

Chitosan (CS) is a cationic linear polysaccharide, which usually exists in the crustaceans of marine arthropods such as shrimp and crab, the crustaceans of insects, the cell membranes of fungi and algae, the shells and bones of molluscs, and the cell walls of higher plants.[11] It is the only natural edible animal fiber with positively charged cationic groups found by humans so far. This amino based cationic property determines its various properties, and has been applied in drug delivery systems.[12] Moreover, CS has a high density of amino groups, which can interact with negatively charged substances such as proteins, solids, dyes and polymers, and has a good effect in water purification.[13] CS has been widely used in drug delivery,[16] gene therapy[17] and tissue engineering[18] due to its biocompatibility,[14] non toxicity, antibacterial activity,[15] biodegradability and many other superior properties. The gel prepared with CS as the matrix is not soluble in water, dilute acid and alkaline solutions, nor in general organic solvents, and has good mechanical strength and chemical stability.

Frontal polymerization (FP) is a way to convert monomers into polymers through local reaction regions, which is mainly used in exothermic reactions. The reaction is carried out by coupling thermal diffusion and Arrhenius reaction kinetics.[19] FP has self propagating property, and can use the heat generated by exothermic reaction to trigger the reaction between components in adjacent regions. Compared with traditional polymerization, the self propagating property of FP provides high conversion in a short time, greatly shortens the reaction time and saves the reaction cost.[20] However, the front-end temperature is difficult to control, and too high a temperature will lead to the "burnout" of the initiator and even the boiling of the monomer, which limits its practical application.[21]

Deep eutectic solvent (DES) is a new kind of almost non-toxic green reagent, which is composed of hydrogen bond acceptor (HBA, such as quaternary ammonium salt) and hydrogen bond

[a]*School of Mechanical Engineering, Wuhan Polytechnic University, Wuhan, Hubei 430023, China. E-mail: libin_027@126.com*

[b]*Wuhan Second Ship Design and Research Institute, Wuhan, 430205, China*

[c]*Hubei Key Laboratory of Theory and Application of Advanced Materials Mechanics, Wuhan University of Technology, Wuhan, Hubei 430070, China*

donor (HBD, such as amide compound) at a certain molar ratio at a certain temperature. According to the amount of HBD, it can be divided into binary and multivariate des. DES was first proposed by Abbott *et al.*,[22] which has a lower melting point than the monomer component. According to the different molar ratio of HBA and HBD, the melting point of the prepared DES is also different. The properties of DES are similar to those of ionic liquids (ILS), but its prep aration is simpler, faster, cheaper and less toxic than that of ILs. In the past five years, des has developed rapidly and its application range has become more and more extensive. When FP is carried out in DES, it can not only act as the monomer of reaction, but also provide a high viscosity environment for the reaction to suppress the convection driven by buoyancy. The various properties of DES can control the inherent reaction of the monomer, so that the monomer can carry out FP at a relatively low temperature.[23] Based on previous studies, we added CS to DES to prepare CS/P(AM-*co*-AA) composite hydrogels. The effect of CS content on the reaction rate of FP was studied. The composite hydrogels were characterized by scanning electron microscopy (SEM) and Fourier transform infrared spectroscopy (FTIR). The effects of CS content on the mechanical properties, pH responsiveness and conductivity of the composite hydrogels were discussed. That is, the polymerizable DES was prepared by mixing ChCl, AA and AM in the molar ratio of 1 : 1 : 1. Then CS was uniformly dispersed in DES, and CS/P(AM-*co*-AA) composite hydrogels were prepared by FP. The effects of different CS contents on the mechanical properties, pH responsiveness and conductivity of the composite hydrogels were studied.

2. Materials and methods

2.1 Materials

N,*N*-Methylene bisacrylamide (MBA) is purchased from Tianjin Cameo Chemical Reagent Co., Ltd and can be used directly. Acrylamide (AM), choline chloride (ChCl), potassium persulfate (KPS), acrylic acid (AA) and chitosan (CS) were all purchased from Shanghai Aladdin Biochemical Technology Co., Ltd. Before use, ChCl needs to be dried in vacuum at 70 °C for two hours to remove the absorbed water. The purity of all reagents is analytical grade.

2.2 Preparation of DES

Take ChCl as HBA, AA and AM as HBD, mix them in a beaker at a molar ratio of 1 : 1 : 1, immerse the beaker in an oil bath at 80 °C (the oil level exceeds the highest point of the mixed reagent), and continuously stir with a glass rod until a transparent and clear liquid is formed. After the prepared DES is allowed to stand for a period of time, different mass fractions of CS are added as shown in Table 1 and stirred until uniform. The formation equation of DES is shown in Fig. 1.

2.3 Preparation of CS/P(AM-*co*-AA) composite hydrogel

At a constant temperature of 35 °C, 0.5 wt% MBA and 0.3 wt% KPS were added to DES and mixed evenly, and then the mixture was transferred to a size of 100 × 12 mm glass test tube, the filling height of the mixture in the test tube is about 80 mm, and the K-type thermocouple is inserted 70 mm below the liquid surface. Use the electric soldering iron to trigger the upper liquid level. After a stable front-end front is formed, evacuate the electric soldering iron and record the change of the front-end position with time. After the reaction, the hydrogel was cooled to room temperature, and the hydrogel was taken out. Finally, the hydrogel was cut into 1–3 mm thick discs, soaked in deionized water for one week, and then lyophilized to constant weight for standby. The FP preparation flow chart is shown in Fig. 2.

Table 1 Composition and proportion of DES

Samples	AA/AM/ChCl (molar ratio)	CS (wt%)	MBA (wt%)	KPS (wt%)
FP0	1 : 1 : 1	0	0.5	0.3
FP1	1 : 1 : 1	1.25	0.5	0.3
FP2	1 : 1 : 1	2.5	0.5	0.3
FP3	1 : 1 : 1	5.0	0.5	0.3
FP4	1 : 1 : 1	10.0	0.5	0.3

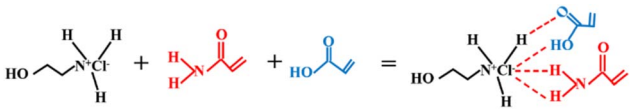

Fig. 1 DES formation equation.

2.4 Performance testing and characterization

2.4.1 Determination of front-end movement rate and temperature. Frontal polymerization reaction generally has a constant front-end moving speed, and the front-end moving speed can be determined by measuring the relationship between the front-end position change and time. In order to monitor the temperature change of the front end, the test tube clamp is clamped at a place 10 mm away from the top of the test tube at room temperature, and the K-type thermocouple connected to the digital thermometer is immersed in the liquid and placed at a position 70 mm away from the liquid surface to measure the temperature at the moving position of the front end.

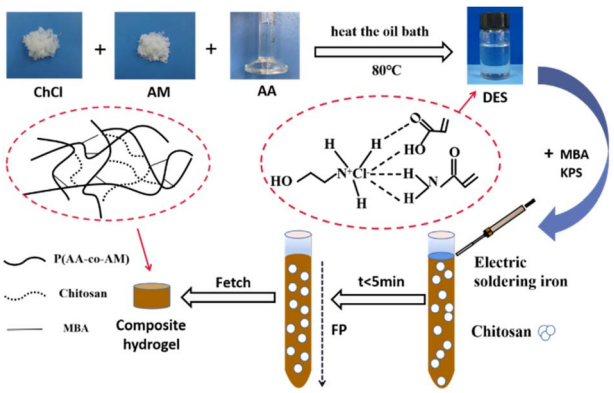

Fig. 2 Schematic diagram of graft polymerization of CS and DES.

2.4.2 SEM characterization. The vacuum freeze-dried samples were sprayed with gold on the cross-section by high vacuum ion sputtering, and then the cross-section micro morphology was observed by scanning electron microscope.

2.4.3 FTIR characterization. The small pieces of dry hydrogel were ground into powder, and then the solid powder samples were mixed with potassium bromide, ground, pressed, and the liquid samples were smeared for FTIR test.

2.4.4 pH response performance test of hydrogel. Prepare buffer solutions with pH of 3, 4.8 (citric acid/sodium citrate) and pH of 9.4, 10.8 (sodium carbonate/sodium bicarbonate), and accurately detect the pH of the buffer solution with a digital pen type pH meter (PH208, accuracy 0.01). Put the dry hydrogel with a mass of about 20 mg into the buffer solution until the swelling is balanced, absorb the water stains on the surface of the hydrogel with filter paper, weigh and record until the weight does not change. The equation for calculating the equilibrium swelling rate (ESR) is as follows:

$$\mathrm{ESR} = \frac{m_t - m_0}{m_0} \quad (1)$$

where, m_0 is the initial weight of the hydrogel, and m_t is the weight of the hydrogel after the water absorption time t.

2.4.5 Tensile and compressive properties test of hydrogel. TA.XTC-18 texture analyzer was used for compression test of hydrogel. Before the test, the hydrogel was cut into a cylindrical shape with a diameter of 10 mm and a length of 10 mm. The compression head was compressed downward at a speed of 3 mm min^{-1} until the hydrogel deformation reached 80%. The tensile properties of the hydrogel samples were tested by the electronic universal testing machine controlled by the microcomputer. The tensile speed was set as 100 mm min^{-1} and the original gauge distance was 50 mm. The calculation formula of the compressive and tensile strength of the hydrogel was as follows:

$$P = \frac{F}{S} \quad (2)$$

where, F is the applied force, unit N; S is the cross-sectional area of the hydrogel, unit m^2.

2.4.6 Conductivity test of hydrogel. A cylindrical hydrogel with a diameter of 10 mm and a length of 10 mm was taken, and the resistance of the cylindrical hydrogel sample was measured by the double electrode method. And the ionic conductivity is calculated according to formula (3).

$$\sigma = \frac{L}{AR_\mathrm{b}} \quad (3)$$

Among σ ($\mathrm{mS\ cm}^{-1}$) represents the conductivity, L represents the length of the hydrogel, R_b represents the impedance, and A is the cross-sectional area of the hydrogel.

3. Results and discussion

3.1 Preparation of CS/P(AM-*co*-AA) composite hydrogel by frontal polymerization

Add CS with different mass fractions into des for stirring to obtain a uniform mixture. After adding KPS, transfer it to the test tube. Heat the top of the test tube with an electric iron until the polymerization front is formed. The reaction proceeds rapidly under the action of KPS, and a large amount of heat is released to continue to initiate the polymerization of monomers. The polymerized monomers continue to exothermically initiate the unreacted monomers, so that the polymerization front rapidly spreads along the test tube at a constant speed until the monomers in the test tube are completely reacted. The time of the whole reaction process does not exceed 7 min.

The temperature and velocity of the polymerization front were measured by a K-type thermocouple. The K-type thermocouple was inserted 70 mm below the liquid surface of the mixed solution, and the temperature change with time during the reaction was recorded. The relationship between the front end position and time during the polymerization of CS hydrogels with different mass fractions is shown in Fig. 3(a). It can be seen from the figure that the relationship between the front end position and time is linear, and the polymerization front moves downward at a constant speed, which indicates that the polymerization reaction does not occur naturally. As can be seen from Fig. 3, with the increase of CS content, the reaction rate gradually increases and the reaction temperature gradually increases. When the CS content is increased from 0 wt% to 10.0 wt%, the front-end speed is increased from 1.30 cm min^{-1} to 1.85 cm min^{-1}, and the front-end temperature is increased from 131.9 °C to 164.8 °C. This is because the presence of AA makes the solution appear weakly acidic, while in the weak acid environment, the β-1-4 glycosidic bond will be slowly hydrolyzed to produce low molecular chitosan,[24] resulting in an increase in the viscosity of DES, an increase in the front temperature of the reaction, and a faster reaction rate.[25]

3.2 Micro morphology analysis of hydrogel

The hydrogel was immersed in deionized water for 7 days to dissolve the soluble substances therein, then pre frozen and freeze-dried in a freeze dryer. The cross-sectional morphology of the dried gel was observed by SEM to study the effect of CS on the internal micro morphology of the hydrogel. As shown in Fig. 4(a), the surface of hydrogel without CS is smooth without pores, while after CS is added, pores appear on the surface of hydrogel, and the pore size of hydrogel gradually increases with the increase of CS content. As shown in Fig. 4(b), the pore size of FP1 is 30 μm. While when the content of CS increased to 10 wt%, the pore size of FP4 in Fig. 4(e) increased to 200 μm.

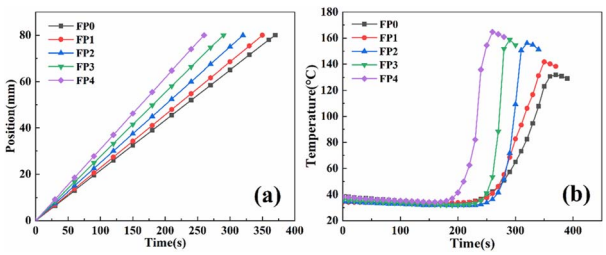

Fig. 3 (a) Front end position time curve and (b) temperature time curve during frontal polymerization.

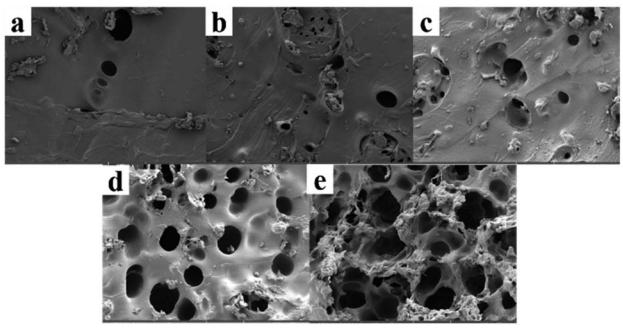

Fig. 4 SEM diagram of FP0 (a), FP1 (b), FP2 (c), FP3 (d) and FP4 (e).

About 6.67 times that of FP1. The drastic change of pore size of hydrogels with different CS content can be attributed to the change of hydrogel cross-linking degree. When CS enters the hydrogel, the amino groups in CS are protonated by hydrogen ions in the acid, resulting in the decrease of cross-linking degree.[26] The cross-linking degree of composite hydrogels gradually decreases with the increase of CS content, resulting in the increase of pore size of hydrogels.[27] The above phenomenon indicates that CS has entered the hydrogel.

3.3 Fourier transform infrared spectroscopy (FTIR)

Fig. 5 shows the infrared spectra of CS, P(AM-*co*-AA) and CS/P(AM-*co*-AA). In the figure, the absorption combination of carboxylate and alcohol's O–H expansion band appears in a wide range of 3500–2550 cm^{-1}.[29] In the spectrum of CS, the bands at 897 cm^{-1} and 1031 cm^{-1} belong to the extension of the pyran ring and C=O bond, and there are two wide absorption bands at 2876 cm^{-1} and 3419 cm^{-1}, the formation of which can be attributed to the stretching vibration of C–H bond and O–H bond.[28] In CS/P(AM-*co*-AA) spectra, bands at 1410 cm^{-1} and 1455 cm^{-1} represent the introduction of functional groups such as –COOH and N–H bonds into the hydrogel. The absorption peak of 1666 cm^{-1} in CS/P(AM-*co*-AA) spectrum is stronger than that at 1668 cm^{-1} in P(AM-*co*-AA) spectrum, which is mainly attributed to the stretching vibration of C=O bond.[30] The above phenomenon indicates that CS/P(AM-*co*-AA) hydrogel has been successfully prepared.

3.4 pH response performance of CS/P(AM-*co*-AA) composite hydrogel

Fig. 6 shows the swelling behavior of P(AM-*co*-AA) and CS/P(AM-*co*-AA) at different pH values. As can be seen from the figure, with the increase of pH value, the swelling rate of the samples showed an increasing trend. When pH = 3, the presence of a large amount of H^+ reduces the COO^- ion content, thus weakening the mutual repulsion between anions. In the absence of sufficient repulsion, the extension of the polymer chain is limited, and the hydrogel has almost no water absorption capacity.[30] However, with the increase of pH value, the hydrogen bond interaction of –COOH group was weakened, and the swelling rate of hydrogel gradually increased. When pH > 4.8, the carboxyl group dissociates, and the amino and carboxylic acid groups are highly repulsive under alkaline conditions,[28] resulting in the increase of the internal osmotic pressure of the hydrogel. A large number of water molecules enter the gel network to balance the osmotic pressure between the internal gel and the external solution, resulting in the increase of the swelling rate of the hydrogel.[31] When the pH continued to rise to 9.8, the swelling rate of hydrogel was slightly decreased compared with that under acidic condition, because the shielding effect of anti-ion (Na^+) in buffer solution restricted the swelling of hydrogel under high pH environment.[32] By comparing the swelling rate of hydrogel at the same pH value, it can be seen that the equilibrium swelling ratio of hydrogel gradually decreases with the increase of CS content, which is because CS is hydrophobic. With the increase of CS content, hydrogel's hydrophilicity decreases, resulting in the decrease of ESR.[33]

3.5 Mechanical properties of CS/P(AM-*co*-AA) composite hydrogel

As shown in Fig. 7, the tensile and compressive curves of CS/P(AM-*co*-AA) composite hydrogel. From the figure, it can be seen

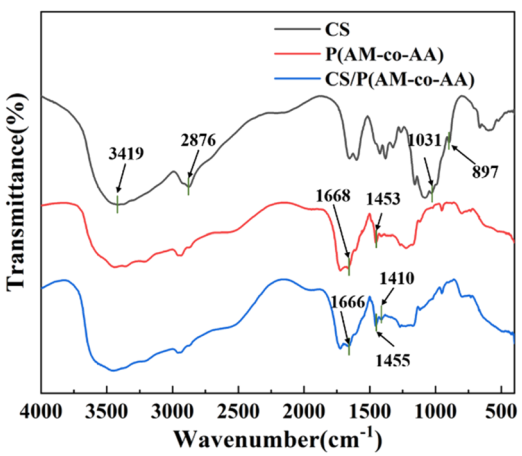

Fig. 5 FTIR of pure CS and CS/P(AM-*co*-AA) composite hydrogels.

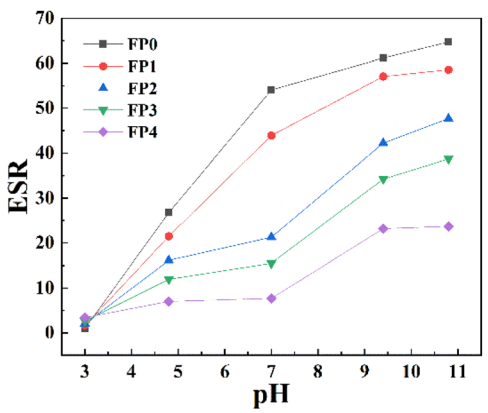

Fig. 6 pH value response curve of CS/P(AM-*co*-AA) composite hydrogel.

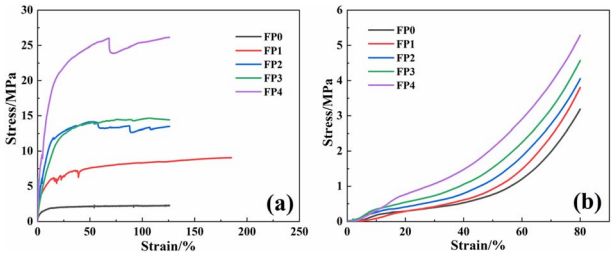

Fig. 7 (a) Tensile curve and (b) compression curve of CS/P(AM-*co*-AA) composite hydrogel.

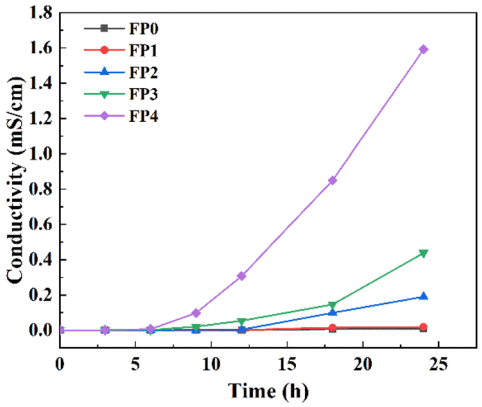

Fig. 8 Conductivity of CS/P(AM-*co*-AA) composite hydrogel.

that FP0 shows low mechanical properties, but with the increase of CS content in the hydrogel, the tensile and compressive strength of the composite hydrogel show an upward trend. It can be seen from Fig. 7(a) that the maximum tensile stress of FP0 is 2.25 mPa, and when the content of CS reaches 10 wt%, the maximum tensile stress of hydrogel increases to 26.13 mPa, which is 11.61 times that of FP0. It can be seen from Fig. 7(b) that the maximum compressive strength of FP0 is 3.19 mPa. After adding CS with a mass fraction of 10 wt%, the maximum compressive strength increases to 5.28 mPa, and the compressive strength increases by 1.65 times. The mechanical properties of the composite hydrogel are significantly increased because the increase of CS concentration will increase the entanglement between hydrogen bonds and molecular chains.[34] The composite hydrogel increases the physical association in the hydrogel through the hydrogen bond generated between the hydroxyl group in AA and the amino group in CS, which enhances the mechanical properties of the hydrogel.[35] At the same time, there is supramolecular interaction between CS and AM segments.[36] Due to the existence of hydrogen bonds and supramolecular interactions, when the hydrogel is destroyed, the polymer chain can be automatically reestablished, which increases the mechanical properties of the hydrogel.

3.6 Conductivity of CS/P(AM-*co*-AA) composite hydrogel

Since CS is a cationic polymer with positive charge, adding CS to hydrogel can enhance the conductivity of hydrogel.[37] CS is also an electrolyte containing amino groups, which can be hydrolyzed to produce hydroxide ions. Hydroxide ions can hydrolyze into cations in water, and the good hydrophilicity of hydrogels can make CS hydrolyze through the water molecules in the gel network, resulting in the increase of the conductivity of hydrogels.[38] Fig. 8 shows the change rule of the conductivity of CS/P(AM-*co*-AA) composite hydrogels with different CS contents when exposed to air over time. It can be seen that the conductivity of the composite hydrogels increases with the passage of time. The reason for this phenomenon is that hydrogels contain hydrophilic ChCl. Good water absorption makes hydrogels continuously absorb moisture from the air during the process of exposure to the air. A large number of water molecules enter the pores of the hydrogel, which makes the transfer of cations in the hydrogel more rapid and thus increases the electrical conductivity.[39] As can be seen from the figure, with the passage of time, the higher the CS content of the hydrogel, the greater the increase of its conductivity, in which the conductivity of FP4 increased from 0.006 mS cm^{-1} to 1.59 mS cm^{-1} after 24 h exposure, an increase of nearly 260 times, and the conductivity of FP4 was nearly 160 times that of FP0. The reason for these phenomena may be that the increase of water molecules leads to more thorough hydrolysis of CS and more cations are hydrolyzed, resulting in higher conductivity of the samples added with CS.

4. Conclusions

In this paper, CS/P(AM-*co*-AA) composite hydrogel was prepared by compounding CS with CHCl AA AM ternary DES, using MBA as crosslinking agent and KPS as initiator, and the structure and properties of the composite hydrogel were studied experimentally. The results showed that:

(1) CS/P(AM-*co*-AA) composite hydrogel has good pH responsiveness, and the composite hydrogel shows excellent responsiveness in alkaline environment, which makes the composite hydrogel have broad application prospects in drug release.

(2) The addition of CS will enhance the entanglement between molecular chains in the composite hydrogel and increase the content of hydrogen bonds in the composite hydrogel. The increase of CS content leads to the increase of the mechanical properties of the composite hydrogel. The maximum tensile strength of the hydrogel with CS content of 10 wt% is 11.61 times that of the hydrogel without CS, and the maximum compressive strength is 1.65 times that of the hydrogel without CS.

(3) CS is a cationic polymer with positive charge. When CS is added to the composite hydrogel as a filler, the conductivity of the hydrogel can be enhanced. When the hydrogel is exposed to the air for 24 h, the conductivity of the hydrogel with CS content of 10 wt% increases nearly 260 times due to the electrolysis of CS.

Author contributions

B. L., proposed the ideas, steps and details of the experiment, most of the experiments were done by W. R. H., M. J. Z, J. Z. L.,

where W. R. H was instrumental in the proper conduct of the experiments and wrote the article together with B. L., and all the authors analyzed the data, discussed the conclusions.

Conflicts of interest

The authors declare that there are no competing interests regarding the publication of this article.

Acknowledgements

The work is supported by 2022 Knowledge Innovation Dawn Special Plan Project (2022010801020393), Marine Defense Technology Innovation Center Innovation Fund (JJ-2020-719-01), Natural Science Foundation of Hubei Province (2021CFB292) and Research and Innovation Initiatives of WHPU (2022J04). This work was finished at Wuhan Polytechnic University, Wuhan.

Notes and references

1 T. Rac, P. Chvs, M. Yamini and C. H. Prasad, *Int. J. Curr. Pharm. Res.*, 2021, **13**(1), 12–17.
2 A. S. Hoffman, *Adv. Drug Delivery Rev.*, 2012, **64**, 18–23.
3 H. Agaba, L. J. Baguma Orikiriza, J. F. Osoto Esegu, J. Obua, J. D. Kabasa and A. Hüttermann, *Clean: Soil, Air, Water*, 2010, **38**(4), 328–335.
4 J. Nam, I.-B. Jung, B. Kim, S.-M. Lee, S.-E. Kim, K.-N. Lee and D.-S. Shin, *Sens. Actuators, B*, 2018, **270**, 112–118.
5 D. Seliktar, *Science*, 2012, **336**(6085), 1124–1128.
6 A. Mateescu, Y. Wang, J. Dostalek and U. Jonas, *Membranes*, 2012, **2**(1), 40–69.
7 K. Haraguchi, H.-J. Li, Y. Xu and G. Li, *Polymer*, 2016, **96**, 94–103.
8 Z. R. Miladinovic, M. Micic and E. Suljovrujic, *J. Polym. Res.*, 2016, **23**, 4.
9 A. Hyder Ali and K. S. V. Srinivasan, *J. Macromol. Sci., Part A: Pure Appl.Chem.*, 1995, **32**(12), 1985–1995.
10 D. Leal, W. De Borggraeve, M. V. Encinas, B. Matsuhiro and R. Muller, *Carbohydr. Polym.*, 2013, **92**(1), 157–166.
11 Q. Li, E. T. Dunn, E. W. Grandmaison and M. F. A. Goosen, *J. Bioact. Compat. Polym.*, 2016, **7**(4), 370–397.
12 A. Bernkop-Schnurch and S. Dunnhaupt, *Eur. J. Pharm. Biopharm.*, 2012, **81**(3), 463–469.
13 A. J. Al-Manhel, A. R. S. Al-Hilphy and A. K. Niamah, *J. Saudi Soc. Agric. Sci.*, 2018, **17**(2), 186–190.
14 S. Rodrigues, M. Dionisio, C. R. Lopez and A. Grenha, *J. Funct. Biomater.*, 2012, **3**(3), 615–641.
15 N. R. Sudarshan, D. G. Hoover and D. Knorr, *Food Biotechnol.*, 1992, **6**(3), 257–272.
16 N. Bhattarai, J. Gunn and M. Zhang, *Adv. Drug Delivery Rev.*, 2010, **62**(1), 83–99.
17 R. Jayakumar, K. P. Chennazhi, R. A. A. Muzzarelli, H. Tamura, S. V. Nair and N. Selvamurugan, *Carbohydr. Polym.*, 2010, **79**(1), 1–8.
18 F. Croisier and C. Jérôme, *Eur. Polym. J.*, 2013, **49**(4), 780–792.
19 J. A. Pojman, G. Curtis and V. M. Ilyashenko, *J. Am. Chem. Soc.*, 1996, **118**(15), 3783–3784.
20 B. Li, J. Liu, D. Fu, Y. Li, X. Xu and M. Cheng, *RSC Adv.*, 2021, **11**(56), 35268–35273.
21 J. D. Mota-Morales, M. C. Gutierrez, I. C. Sanchez, G. Luna-Barcenas and F. del Monte, *Chem. Commun.*, 2011, **47**(18), 5328–5330.
22 A. P. Abbott, G. Capper, D. L. Davies, R. K. Rasheed and V. Tambyrajah, *Chem. Commun.*, 2003, **1**, 70–71.
23 J. D. Mota-Morales, M. C. Gutiérrez, M. L. Ferrer, I. C. Sanchez, E. A. Elizalde-Peña, J. A. Pojman, F. D. Monte and G. Luna-Bárcenas, *J. Polym. Sci., Part A: Polym. Chem.*, 2013, **51**(8), 1767–1773.
24 J. Zhang and L.-w. Song, *J. Clin. Rehabil. Tissue Eng. Res.*, 2011, **15**, 2213–2216.
25 K. F. Fazende, D. P. Gary, J. D. Mota-Morales and J. A. Pojman, *Macromol. Chem. Phys.*, 2020, **221**(6), 1900511.
26 M. Fwu-Long, S. Hsing-Wen and S. Shin-Shing, *Carbohydr. Polym.*, 2002, **48**(1), 61–72.
27 L. Wei, J. Tan, L. Li, H. Wang and S. Liu, *Int. J. Mol. Sci.*, 2022, **23**(3), 1249.
28 G. R. Mahdavinia, A. Pourjavadi, H. Hosseinzadeh and M. J. Zohuriaan, *Eur. Polym. J.*, 2004, **40**(7), 1399–1407.
29 S. Bashir, Y. Y. Teo, S. Naeem, S. Ramesh and K. Ramesh, *PLoS One*, 2017, **12**(7), e0179250.
30 G. He, W. Ke, X. Chen, Y. Kong, H. Zheng, Y. Yin and W. Cai, *React. Funct. Polym.*, 2017, **111**, 14–21.
31 S. Saber-Samandari, M. Gazi and E. Yilmaz, *Polym. Bull.*, 2011, **68**(6), 1623–1639.
32 M. Tally and Y. Atassi, *J. Polym. Res.*, 2015, **22**, 9.
33 A. Martinez-Ruvalcaba, J. C. Sanchez-Diaz, F. Becerra, L. E. Cruz-Barba and A. Gonzalez-Alvarez, *eXPRESS Polym. Lett.*, 2009, **3**(1), 25–32.
34 S. Aihua, X. Dai and Z. Jing, *Polym. Sci., Ser. A*, 2020, **62**(3), 228–239.
35 Y. Jiang, X. Meng, Z. Wu and X. Qi, *Carbohydr. Polym.*, 2016, **144**, 245–253.
36 Y. Liu, D. Xu, Y. Ding, X. Lv, T. Huang, B. Yuan, L. Jiang, X. Sun, Y. Yao and J. Tang, *J. Mater. Chem. B*, 2021, **9**(42), 8862–8870.
37 Y. Ou and M. Tian, *J. Mater. Chem. B*, 2021, **9**(38), 7955–7971.
38 B. Guo, J. Qu, X. Zhao and M. Zhang, *Acta Biomater.*, 2019, **84**, 180–193.
39 H. Ding, X. Liang, Q. Wang, M. Wang, Z. Li and G. Sun, *Carbohydr. Polym.*, 2020, **248**, 116797.